Effective chiral symmetry restoration for heavy-light mesons

V. K. Sazonov,[*] G. Schaffernak, and R. F. Wagenbrunn

Institute of Physics, University of Graz, Universitätsplatz 5, A-8010 Graz, Austria

We study the spectrum of heavy-light mesons within a model with linear instantaneous confining potential. The single-quark Green function and spontaneous breaking of chiral symmetry are obtained from the Schwinger-Dyson (gap) equation. For the meson spectrum we derive a Bethe-Salpeter equation. We solve this equation numerically in the heavy-light limit and obtain effective restoration of chiral and $U(1)_A$ symmetries at large spins.

I. INTRODUCTION

Confinement and chiral symmetry belong to the most important properties of low-energy QCD. On the classical level the massless QCD Lagrangian is invariant under the $U(2)_L \times U(2)_R = SU(2)_R \times SU(2)_L \times U(1)_A \times U(1)_V$ group of chiral symmetry [1]. However, the $SU(2)_A$ and $U(1)_A$ parts of chiral symmetry are dynamically broken. The $U(1)_A$ symmetry is also broken by a quantum anomaly [2–4].

Dynamical symmetry breaking is responsible for the mass generation of low-lying hadrons. For instance, from the chiral symmetry point of view the pion is a pseudo-Goldstone boson associated with the spontaneous broken axial part of chiral symmetry [5]. On the other hand, recent lattice simulations demonstrated the existence of hadrons, even when chiral symmetry is artificially restored [6–8]. This implies that it is not only the breaking of chiral symmetry that contributes to the hadron masses. At the same time excited hadrons can be arranged in the approximate multiplets of chiral and $U(1)_A$ groups [9–15] and this may be considered as an indication of effective restoration of chiral symmetry [16]. However, such effective restoration still requires further experimental confirmation, which involves a discovery of missing hadronic states.

In the case of effective restoration, the system does not undergo a phase transition and the chiral order parameter does not vanish. This means that the quark condensate of the vacuum still persists, but becomes unimportant. This may be understood considering the quarks in the meson rest frame. In hadrons with large spins the quarks have a little probability to be in a state with low momentum and thus they decouple from the quark condensate.

The phenomenon of effective chiral symmetry restoration has been illustrated in [17] within the chirally symmetric confined model [18,19]. This effect has been

proven analytically and by the direct calculations of the meson spectra in the heavy-light case for the quadratic potential [20] and in the light-light case for the linear potential [21,22]. The effective restoration has also been discussed within different approaches in [23–29]. In this work we consider the heavy-light limit of the system of two quarks with masses m_1 and m_2, confined by a linear potential. Such potential is observed in Coulomb gauge lattice simulations [30] and can be considered as the most realistic one from the phenomenological point of view. In the case of massless quarks, the Hamiltonian (3) obeys $SU(2)_L \times SU(2)_R \times U(1)_A \times U(1)_V$ symmetry.

When the mass of the heavy quark $m_2 \to \infty$, the spin and the isospin of the heavy quark and the total angular momentum j_l of the light quark are separately conserved [31–34]. Heavy quark symmetry, which unifies the heavy spin and heavy flavor symmetries, leads to independent dynamics of the light quark with respect to the isospin and spin of the heavy quark. All mesonic states can be classified by quantum numbers of the light quark. For the fixed total angular momentum $j_l \neq 0$, heavy spin symmetry implies the existence of degenerate states with total spin $J = j_l \pm \frac{1}{2}$. In Fig. 1 we present a general view of the spectrum respecting heavy spin symmetry. The heavy flavor symmetry leads to a doubling of all states in the spectrum, because of the two possible orientations of the heavy quark isospin, i.e., each line in Fig. 1 should be considered as an isospin doublet. The bare interaction in the model (3) is isospin independent. It is also isospin independent in all orders of perturbation theory, since we perform all computations in the large N_c approximation, where all fermion loops are suppressed. This leads to a doubling of all states in the spectrum also with respect to the light quark isospin projections.

In the case of the heavy-light system $m_1 = 0$, $m_2 \to \infty$, at large angular momenta the restoration of chiral and $U(1)_A$ symmetries of the light quark is expected. The chiral properties of mesons are defined by the representations of the parity-chiral group [16], consistent with left and right isospins (I_L, I_R) and with J^P quantum numbers. The isospin of the heavy quark doesn't influence the dynamics

---
[*]Also at the Department of Theoretical Physics, St. Petersburg State University, Uljanovskaja 1, St. Petersburg, Petrodvorez 198504, Russia.
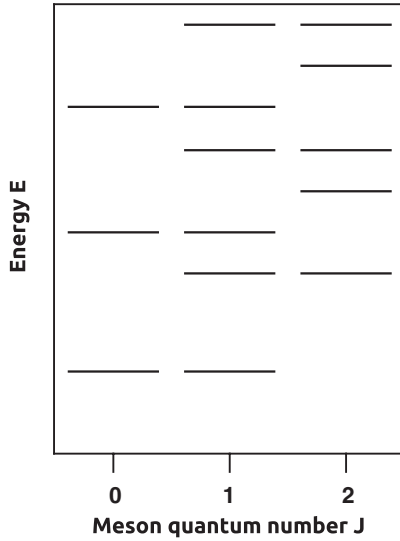vasily.sazonov@uni-graz.at; vasily.sazonov@gmail.com

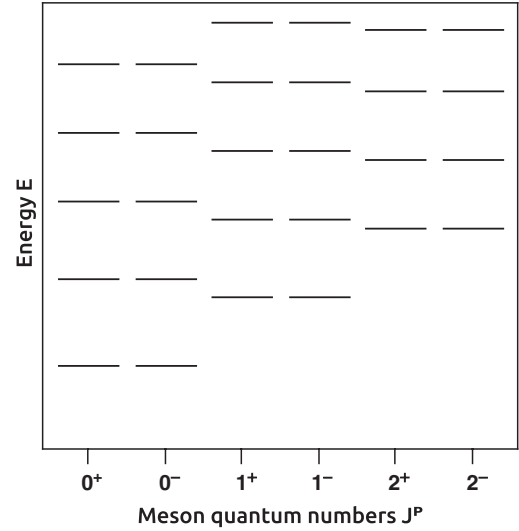FIG. 1.   Expected spectrum for heavy spin symmetry.

FIG. 2.   Expected spectrum given chiral symmetry restoration for the light quark.
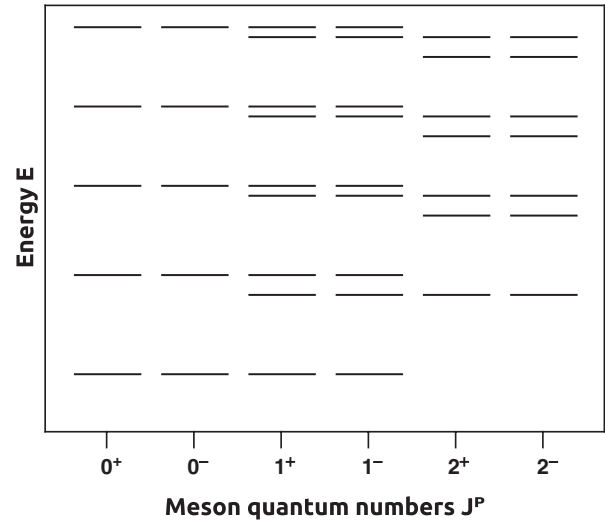
FIG. 3.   Expected spectrum for heavy spin symmetry and chiral symmetry.

of the light quark, so the only possible representation of the parity-chiral group for the heavy-light mesons is

$$(I_L, I_R) \oplus (I_R, I_L) = (1/2, 0) \oplus (0, 1/2), \qquad (1)$$

where $1/2$ is the isospin of the light quark, and the direct sum of two irreducible representations forms a state of well-defined parity. The possible mesons for this representations are

$$I_{\text{light}} = 1/2, J^P = (j_l \pm 1/2)^+$$
$$\leftrightarrow I_{\text{light}} = 1/2, J^P = (j_l \pm 1/2)^-. \qquad (2)$$

The sign $\leftrightarrow$ connects the states which must be degenerate in the chirally symmetric mode. Therefore, the restoration of chiral symmetry implies the appearance of parity doublets. The general view of the meson spectrum with restored chiral symmetry is shown in Fig. 2. Combining the heavy spin and chiral symmetry one comes to the expected spectrum for the heavy-light system in the chiral mode, Fig. 3.

In the following sections within a framework of the chirally symmetric model with the linear confining potential [18,19] we study the aspects of effective restoration of chiral symmetry in heavy-light mesons.

The paper is organized as follows. In Sec. II we describe the model Hamiltonian and the confining potential. Section III is dedicated to chiral symmetry breaking in the vacuum in the considered model. We derive the Bethe-Salpeter equation for heavy-light mesons and show the appearance of the heavy spin symmetry in Sec. IV. In Sec. V we demonstrate the cancellations of the infrared divergences in the Bethe-Salpeter equation. Numerical results for the meson spectrum and for the corresponding wave functions are presented in Secs. VI and VII,

respectively. In Sec. VIII we discuss effective restoration of chiral symmetry and properties of the BSE without the spontaneous breaking of chiral symmetry. We conclude in Sec. IX.

II. CHIRALLY SYMMETRIC MODEL WITH CONFINEMENT

To study effective restoration of chiral symmetry, one has to choose a confining model with spontaneously broken chiral symmetry in $3 + 1$ dimensions. The latter remark is of great importance, since effective chiral symmetry restoration doesn't appear in $1 + 1$ dimensions, because of the absence of rotational motion and spin. Here we consider a model [18,19] which may be viewed as a straight-forward

generalization to the $3 + 1$ dimensional case of the $1 + 1$ dimensional 't Hooft model [35,36]. It was intensively studied in the context of chiral symmetry breaking [37] and chiral properties of hadronic states [20,21,24].

The Hamiltonian of the model is based on the instantaneous current-current interaction with linear potential of the Coulomb type,

$$\hat{H} = \int d^3x \bar{\psi}_i(\vec{x}, t)(-i\vec{\gamma} \cdot \vec{\nabla} + m_i)\psi_i(\vec{x}, t)$$
$$+ \frac{1}{2} \int d^3x d^3y J_\mu^a(\vec{x}, t) K_{\mu\nu}^{ab}(\vec{x} - \vec{y}) J_\nu^b(\vec{y}, t), \quad (3)$$

where $i = 1, 2$ represents a summation over two different quark masses and quark fields $\psi_i = (u_i, d_i)$. The quark current is $J_\mu^a(\vec{x}, t) = \bar{\psi}_i(\vec{x}, t)\gamma_\mu \frac{\lambda^a}{2} \psi_i(\vec{x}, t)$ and the potential looks like

$$K_{\mu\nu}^{ab}(\vec{x} - \vec{y}) = g_{\mu 0} g_{\nu 0} \delta^{ab} V(|\vec{x} - \vec{y}|), \quad (4)$$

where a, b and μ, ν are color and Lorentz indices, respectively.

In the case of two massless quarks, the Hamiltonian obeys $SU(2)_L \times SU(2)_R \times U(1)_A \times U(1)_V$ symmetry for both quarks. When $m_1 = 0$ and $m_2 \neq 0$ the symmetry $SU(2)_L \times SU(2)_R \times U(1)_A \times U(1)_V$ is applicable only to the first quark. For further calculations we absorb the color Casimir factor in the string tension σ

$$\frac{\lambda^a \lambda^a}{4} V(r) = \sigma r. \quad (5)$$

The Fourier transformation of the linear potential is ill defined and requires an infrared regularization. The regularization should be removed, or equivalently the infrared limit should be taken in the final result. All physical observables must be finite in this limit and independent of how the potential was regularized. At the same time, the single quark Green function can be divergent in the infrared limit, which demonstrates that a single quark cannot be observed within the framework of the considered and manifestly confined model.

There exists an infinite amount of physically equivalent regularizations. Following [38], we define the potential as

$$V(p) = \frac{8\pi\sigma}{(p^2 + \mu_{IR}^2)^2}. \quad (6)$$

With the given prescription one can solve the Schwinger-Dyson (gap) and Bethe-Salpeter equations, since all integrals in them are well defined. In the case of the linear potential there are no ultraviolet divergences. For other kinds of potentials the ultraviolet regularization and renormalization might be necessary. For instance, this is the case if the Coulomb interaction is added. In the following we restrict ourselves only to the linear potential.

III. CHIRAL SYMMETRY BREAKING AND THE GAP EQUATION

The interaction with gluon fields (or in our case self interaction via confining potential) leads to the dressing of the Dirac operator,

$$D(p_0, \vec{p}) = iS^{-1}(p_0, \vec{p}) = D_0(p_0, \vec{p}) - \Sigma(p_0, \vec{p}), \quad (7)$$

where $\Sigma(p_0, \vec{p})$ is the quark self-energy and the bare Dirac operator is

$$D_0(p_0, \vec{p}) = p_0 \gamma_0 - \vec{p} \cdot \vec{\gamma} - m. \quad (8)$$

For an instantaneous interaction the self-energy,

$$i\Sigma(\vec{p}) = \int \frac{d^4q}{(2\pi)^4} V(|\vec{p} - \vec{q}|) \gamma_0 \frac{1}{iS_0^{-1}(q_0, \vec{q}) - \Sigma(\vec{q})} \gamma_0, \quad (9)$$

is independent of the energy p_0. Representing the self-energy in terms of Lorentz-invariant amplitudes,

$$\Sigma(\vec{p}) = A(p) - m + \vec{\gamma} \cdot \hat{p}(B(p) - p), \quad (10)$$

and combining Eqs. (7) and (9) we arrive at a system of two coupled integral equations

$$A(p) = m + \frac{1}{2} \int \frac{d^3q}{(2\pi)^3} V(|\vec{p} - \vec{q}|) \frac{A(q)}{\omega_q},$$
$$B(p) = p + \frac{1}{2} \int \frac{d^3q}{(2\pi)^3} V(|\vec{p} - \vec{q}|) \frac{B(q)}{\omega_q} \hat{p} \cdot \hat{q}, \quad (11)$$

where

$$\omega_p = \sqrt{A(p)^2 + B(p)^2} \quad (12)$$

is the single quark energy. Introducing a Bogoliubov (chiral) angle

$$\sin \varphi_p \equiv \frac{A(p)}{\omega_p}, \qquad \cos \varphi_p \equiv \frac{B(p)}{\omega_p} \quad (13)$$

one can reduce the system (11) to a single integral equation,

$$p \sin \varphi_p - m \cos \varphi_p$$
$$= \frac{1}{2} \int \frac{d^3q}{(2\pi)^3} \{V(|\vec{p} - \vec{q}|)$$
$$\cdot (\sin \varphi_q \cos \varphi_p - \hat{p} \cdot \hat{q} \sin \varphi_p \cos \varphi_q)\}. \quad (14)$$

Then the expressions for the amplitudes $A(p)$ and $B(p)$ become

$$A(p) = m + \frac{1}{2} \int \frac{d^3q}{(2\pi)^3} V(|\vec{p} - \vec{q}|) \sin\varphi_q, \quad (15)$$

$$B(p) = p + \frac{1}{2} \int \frac{d^3q}{(2\pi)^3} V(|\vec{p} - \vec{q}|) \hat{p} \cdot \hat{q} \cos\varphi_q \quad (16)$$

and the single quark energy can be determined via

$$\omega_p = p \cos\varphi_p + m \sin\varphi_p$$
$$+ \frac{1}{2} \int \frac{d^3q}{(2\pi)^3} \{ V(|\vec{p} - \vec{q}|)$$
$$\cdot (\sin\varphi_q \sin\varphi_p + \hat{p} \cdot \hat{q} \cos\varphi_p \cos\varphi_q) \}. \quad (17)$$

The single quark energy

$$\omega_p = \frac{\sigma}{2\mu_{IR}} + \omega_p^f \quad (18)$$

as the energy of any color state is infinite in the infrared limit. The energies of all color-singlet states are finite and well defined. This is the manifestation of confinement within the considered model.

At the same time, the integral in (14) converges at $p = q$, since the infrared divergence of the potential exactly cancels in the sum of the two integrand terms. Consequently, the chiral angle and the dynamical mass

$$M(p) = p \tan\varphi_p \quad (19)$$

are finite and can be found by the numerical solution of the gap equation (14). This solution leads to the nonzero quark condensate,

$$\langle \bar{q}q \rangle = -\frac{N_c}{\pi^2} \int_0^\infty dp\, p^2 \sin\varphi_p = -0.012\sigma^{3/2}, \quad (20)$$

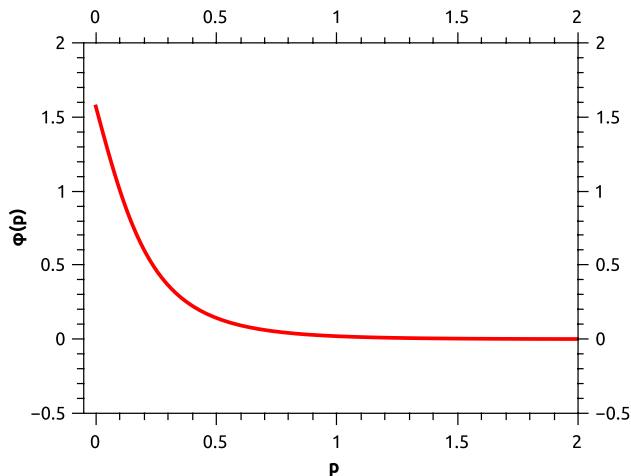which signals spontaneous breaking of chiral symmetry. As seen from the Fig. 4 and Fig. 5, the effect of chiral

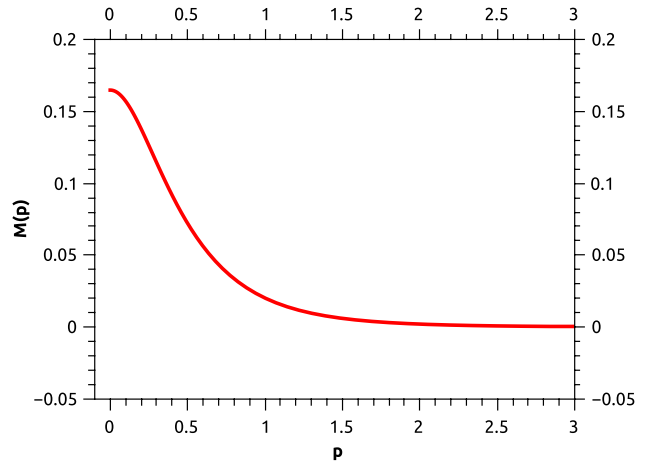FIG. 4 (color online).   Chiral angle solution for m = 0.

FIG. 5 (color online).   Dynamical mass function, momentum in units of $\sqrt{\sigma}$.

symmetry breaking is large at low momenta. At large momenta these functions both approach zero. This property of the chiral angle is crucial for the understanding of effective chiral symmetry restoration.

IV. BETHE-SALPETER EQUATION FOR THE HEAVY-LIGHT SYSTEM

To describe a bound state of quarks and antiquarks we use the homogeneous Bethe-Salpeter equation (BSE) in the meson rest frame

$$\chi(P, p) = -i \int \frac{d^4q}{(2\pi)^4} K(P, p, q) S_1\left(q + \frac{P}{2}\right)$$
$$\cdot \chi(P, q) S_2\left(q - \frac{P}{2}\right), \quad (21)$$

where P is the mesons total momentum, p is the relative momentum and q is the loop momentum that has to be integrated over, S_1 and S_2 are the propagators for the quark and anti-quark. $K(P, p, q)$ is the Bethe-Salpeter kernel and finally χ is the meson vertex function. In the rest frame of the meson the total momentum becomes

$$P^\nu = (m, 0, 0, 0), \quad (22)$$

with m being the mass of the bound-state. For the model with instantaneous interaction, the amplitude is energy independent and in the ladder approximation the equation reads

$$\chi(m, \vec{q}) = -i \int \frac{d^4q}{(2\pi)^4} V(|\vec{p} - \vec{q}|) \gamma_0 S_1\left(q_0 + \frac{m}{2}, \vec{q}\right)$$
$$\cdot \chi(m, \vec{q}) S_2\left(q_0 - \frac{m}{2}, \vec{q}\right) \gamma_0. \quad (23)$$

To solve the Bethe-Salpeter equation (23) we expand the meson vertex function $\chi(m, \vec{q})_{JM}^P$ into a set of all possible

independent Poincaré invariant amplitudes consistent with J^P quantum numbers (see Appendix A). The mesons constructed from two quarks with different masses can be grouped in two categories:

$$A:\begin{cases} J^-, J = 2n \\ J^+, J = 2n + 1 \end{cases} \qquad B:\begin{cases} J^+, J = 2n \\ J^-, J = 2n + 1. \end{cases}$$

In Appendix B we rewrite the BSE for two different quark masses m_1 and m_2 as systems of coupled integral equations, where each system corresponds to a certain category of mesons. For each value of J the categories A and B contain chiral partners, hence when chiral symmetry is effectively restored, the equations for both categories must coincide.

To derive the Bethte-Salpeter equations for the heavy-light mesons we assume $m_1 = 0$ and $m_2 \to \infty$. The latter limit means that the heavy quark chiral angle becomes constant $\varphi_2 \to \frac{\pi}{2}$. To shorten notations we denote the light quark chiral angle φ_1 as φ and

$$r_+ = \sqrt{(1 + \sin\varphi(p))(1 + \sin\varphi(q))}$$
$$r_- = \sqrt{(1 - \sin\varphi(p))(1 - \sin\varphi(q))}$$
$$\int_q := \frac{1}{2}\int\frac{d^3q}{(2\pi)^3}V(k)$$
$$\vec{\psi}(p) = (\psi_1(p), \psi_2(p)). \tag{24}$$

The mass of the whole meson can be splitted into the mass of the heavy quark and the binding energy $\epsilon = m - m_2$. The heavy quark energy is replaced by $\omega_2(p) \to m_2 + \frac{\sigma}{2\mu_{IR}}$, where the last term is the corresponding infrared divergence. All wave functions, propagating backwards in time, vanish in the heavy-light limit, when the interaction is instantaneous [20]. The remaining wave functions for the forward motion in time are identified as $\psi_{i,+} \equiv \psi_i$ (see Appendix C).

Equations for category A for $J > 0$ become

$$\left(\omega(p) + \frac{\sigma}{2\mu_{IR}} - \epsilon\right)\psi_1(p) = \int_q\left\{\left[r_+P_J(\hat{p}\cdot\hat{q}) + r_-\frac{(J+1)P_{J+1}(\hat{p}\cdot\hat{q}) + JP_{J-1}(\hat{p}\cdot\hat{q})}{2J+1}\right]\psi_1(q)\right.$$
$$\left. + r_-\frac{\sqrt{J(J+1)}}{2J+1}[P_{J+1}(\hat{p}\cdot\hat{q}) - P_{J-1}(\hat{p}\cdot\hat{q})]\psi_2(q)\right\},$$
$$\left(\omega(p) + \frac{\sigma}{2\mu_{IR}} - \epsilon\right)\psi_2(p) = \int_q\left\{\left[r_+P_J(\hat{p}\cdot\hat{q}) + r_-\frac{JP_{J+1}(\hat{p}\cdot\hat{q}) + (J+1)P_{J-1}(\hat{p}\cdot\hat{q})}{2J+1}\right]\psi_2(q)\right.$$
$$\left. + r_-\frac{\sqrt{J(J+1)}}{2J+1}[P_{J+1}(\hat{p}\cdot\hat{q}) - P_{J-1}(\hat{p}\cdot\hat{q})]\psi_1(q)\right\}, \tag{25}$$

and for $J = 0$ there is only one equation,

$$\left(\omega(p) + \frac{\sigma}{2\mu_{IR}} - \epsilon\right)\psi_1(p) = \int_q[r_+ + r_-\hat{p}\cdot\hat{q}]\psi_1(q). \tag{26}$$

Equations for category B for $J > 0$ become

$$\left(\omega(p) + \frac{\sigma}{2\mu_{IR}} - \epsilon\right)\psi_1(p) = \int_q\left\{\left[r_-P_J(\hat{p}\cdot\hat{q}) + r_+\frac{JP_{J+1}(\hat{p}\cdot\hat{q}) + (J+1)P_{J-1}(\hat{p}\cdot\hat{q})}{2J+1}\right]\psi_1(q)\right.$$
$$\left. + r_+\frac{\sqrt{J(J+1)}}{2J+1}[P_{J+1}(\hat{p}\cdot\hat{q}) - P_{J-1}(\hat{p}\cdot\hat{q})]\psi_2(q)\right\}, \tag{27}$$
$$\left(\omega(p) + \frac{\sigma}{2\mu_{IR}} - \epsilon\right)\psi_2(p) = \int_q\left\{\left[r_-P_J(\hat{p}\cdot\hat{q}) + r_+\frac{(J+1)P_{J+1}(\hat{p}\cdot\hat{q}) + JP_{J-1}(\hat{p}\cdot\hat{q})}{2J+1}\right]\psi_2(q)\right.$$
$$\left. + r_+\frac{\sqrt{J(J+1)}}{2J+1}[P_{J+1}(\hat{p}\cdot\hat{q}) - P_{J-1}(\hat{p}\cdot\hat{q})]\psi_1(q)\right\} \tag{28}$$

and for $J = 0$ the equation is

$$\left(\omega(p) + \frac{\sigma}{2\mu_{IR}} - \epsilon\right)\psi_2(p) = \int_q[r_- + r_+\hat{p}\cdot\hat{q}]\psi_2(q). \tag{29}$$

The given heavy-light equations exhibit heavy-quark spin symmetry, which involves a degeneration of states with fixed parity and $J = j_l \pm \frac{1}{2}$. To prove heavy spin symmetry, we diagonalize the Eqs. (25)–(29). Symbolically, the matrix equations for categories A and B read

$$C\vec{\psi}(p) = D\vec{\psi}(q), \qquad (30)$$

with C already being in diagonal form for both categories,

$$C = C_A = C_B = \begin{pmatrix} \omega(p) + \frac{\sigma}{2\mu_{IR}} - \epsilon & 0 \\ 0 & \omega(p) + \frac{\sigma}{2\mu_{IR}} - \epsilon \end{pmatrix}. \qquad (31)$$

Matrix D is different for categories A and B and given by

$$D_A = \begin{pmatrix} \int_q \left(r_+ P_J + r_- \frac{(J+1)P_{J+1}(\hat{p}\cdot\hat{q}) + J P_{J-1}(\hat{p}\cdot\hat{q})}{2J+1} \right) & \int_q \left(r_- \frac{\sqrt{J(J+1)}}{2J+1} [P_{J+1}(\hat{p}\cdot\hat{q}) - P_{J-1}(\hat{p}\cdot\hat{q})] \right) \\ \int_q \left(r_- \frac{\sqrt{J(J+1)}}{2J+1} [P_{J+1}(\hat{p}\cdot\hat{q}) - P_{J-1}(\hat{p}\cdot\hat{q})] \right) & \int_q \left(r_+ P_J + r_- \frac{J P_{J+1}(\hat{p}\cdot\hat{q}) + (J+1)P_{J-1}(\hat{p}\cdot\hat{q})}{2J+1} \right) \end{pmatrix}$$

$$D_B = \begin{pmatrix} \int_q \left(r_- P_J + r_+ \frac{J P_{J+1}(\hat{p}\cdot\hat{q}) + (J+1)P_{J-1}(\hat{p}\cdot\hat{q})}{2J+1} \right) & \int_q \left(r_+ \frac{\sqrt{J(J+1)}}{2J+1} [P_{J+1}(\hat{p}\cdot\hat{q}) - P_{J-1}(\hat{p}\cdot\hat{q})] \right) \\ \int_q \left(r_+ \frac{\sqrt{J(J+1)}}{2J+1} [P_{J+1}(\hat{p}\cdot\hat{q}) - P_{J-1}(\hat{p}\cdot\hat{q})] \right) & \int_q \left(r_- P_J + r_+ \frac{(J+1)P_{J+1}(\hat{p}\cdot\hat{q}) + J P_{J-1}(\hat{p}\cdot\hat{q})}{2J+1} \right) \end{pmatrix}. \qquad (32)$$

D_A and D_B can be transformed into diagonal form

$$D_A = \begin{pmatrix} \int_q (r_- P_{J-1} + r_+ P_J) & 0 \\ 0 & \int_q (r_- P_{J+1} + r_+ P_J) \end{pmatrix} \qquad D_B = \begin{pmatrix} \int_q (r_+ P_{J-1} + r_- P_J) & 0 \\ 0 & \int_q (r_+ P_{J+1} + r_- P_J) \end{pmatrix}. \qquad (33)$$

For the case $J = 0$ the matrices C are

$$C_A^{J=0} = C_B^{J=0} = \omega(p) + \frac{\sigma}{2\mu_{IR}} - \epsilon \qquad (34)$$

and the matrices D are

$$D_A^{J=0} = \int_q (r_+ P_0 + r_- P_1)$$

$$D_B^{J=0} = \int_q (r_+ P_1 + r_- P_0). \qquad (35)$$

For each $J > 0$ the spectrum of J^- consists of one part that coincides with $(J-1)^-$ and one part that coincides with $(J+1)^-$. The same is true for positive parity solutions, what finishes the proof of the heavy quark spin symmetry.

V. INFRARED PROPERTIES OF THE BETHE-SALPETER EQUATION

It is crucially to note that all infrared divergences, appearing in functions $A(p)$, $B(p)$ and $\omega(p)$ in the limit $\mu_{IR} \to 0$, exactly cancel in all BS equations. This ensures the existence of finite solutions for the binding energy spectrum and meson wave functions. Here we demonstrate the cancellation on the example of the $J = 0$ equation for category A (26).

Using the representation for the Dirac delta function,

$$\lim_{\mu_{IR} \to 0} \frac{\mu_{IR}}{\pi^2} \int d^3 q \frac{1}{((\vec{p} - \vec{q})^2 + \mu_{IR}^2)^2} f(\vec{q})$$

$$= \int d^3 q \, \delta(\vec{p} - \vec{q}) f(\vec{q}) = f(\vec{p}), \qquad (36)$$
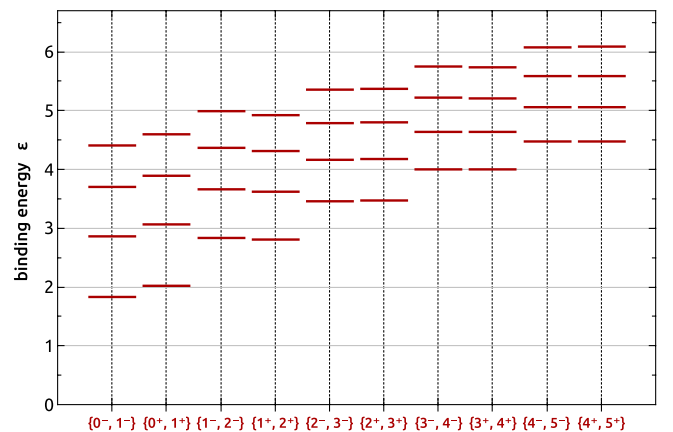
for $\mu_{IR} \to 0$ from Eq. (26) we obtain

FIG. 6 (color online). Heavy-light meson binding energy in units of $\sqrt{\sigma}$.

TABLE I.   Orbital, j_l, heavy-light meson binding energy.

$0+\frac{1}{2}$ $\{0^-,1^-\}$	$1-\frac{1}{2}$ $\{0^+,1^+\}$	$2-\frac{1}{2}$ $\{1^-,2^-\}$	$1+\frac{1}{2}$ $\{1^+,2^+\}$	$2+\frac{1}{2}$ $\{2^-,3^-\}$	$3-\frac{1}{2}$ $\{2^+,3^+\}$	$4-\frac{1}{2}$ $\{3^-,4^-\}$	$3+\frac{1}{2}$ $\{3^+,4^+\}$	$4+\frac{1}{2}$ $\{4^-,5^-\}$	$5-\frac{1}{2}$ $\{4^+,5^+\}$
1.84	2.04	2.84	2.82	3.47	3.48	4.02	4.02	4.49	4.49
2.87	3.08	3.67	3.63	4.18	4.19	4.65	4.65	5.07	5.07
3.71	3.91	4.38	4.32	4.80	4.82	5.23	5.22	5.60	5.60
4.42	4.61	5.01	4.94	5.37	5.39	5.76	5.75	6.09	6.10

$$\frac{\sigma}{\mu_{IR}}\psi_1(p) = \frac{1}{2}\int\frac{d^3q}{(2\pi)^3}8\pi\sigma\frac{\pi^2\delta(\vec{p}-\vec{q})}{\mu_{IR}}$$
$$\cdot\,[(1+\sin\varphi(p))$$
$$+\,(1-\sin\varphi(p))\hat{p}\cdot\hat{p}]\psi_1(p). \qquad (37)$$

The relation (37) is an identity and proofs the cancellation of infrared divergences in the BSE.

VI. NUMERICAL RESULTS FOR THE SPECTRUM

The diagonalized equations (33) may be solved numerically (see Appendix D). In Fig. 6 we present results for the binding energy spectrum of the heavy-light mesons. Collecting the values for the heavy-quark spin multiplets, in Table I we show explicitly the orbital and spin quantum numbers for the light quark $j_l = l + s$, as well as the corresponding heavy-spin multiplet for the meson.

The energy gap between opposite parity members of the same chiral multiplet, generated by chiral symmetry breaking, goes rapidly to zero with increasing angular momentum, see Table II. In Fig. 7 the angular Regge trajectories for the ground states of chiral partners are shown. The trajectories exhibit asymptotically linear behavior and coincide with each other. These numerical results prove the effective chiral symmetry restoration for the heavy-light mesons at large angular momenta for the considered model. On the contrary the radial Regge trajectories do not coincide, see Fig. 8. This demonstrates that the phenomenon of effective chiral restoration is strongly related to the angular momentum. For instance, it cannot appear in $1 + 1$ dimensions [39] because of the absence of the rotational motion.

VII. WAVE FUNCTIONS

Since the spectrum exhibits the effective restoration of chiral symmetry, it must be seen also at the level of wave functions. Continuing the classification of the states with respect to the total angular momentum of the light quark,

TABLE II.   Energy gap between opposite parity members of the same chiral multiplet.

Spin multiplet	$\{0,1\}$	$\{1,2\}$	$\{2,3\}$	$\{3,4\}$	$\{4,5\}$
Ground state gap	0.20	0.02	0.01	0.00	0.00

we compare the chiral partners' ground state wave functions for different values of j_l. As can be seen from the respective plots, the ground state multiplets with $j_l = \frac{1}{2}$ have different wave function shapes, while for $j_l = \frac{3}{2}$ the wave functions are much closer to each other and they practically coincide for $j_l = \frac{7}{2}$, see Figures 9–11.
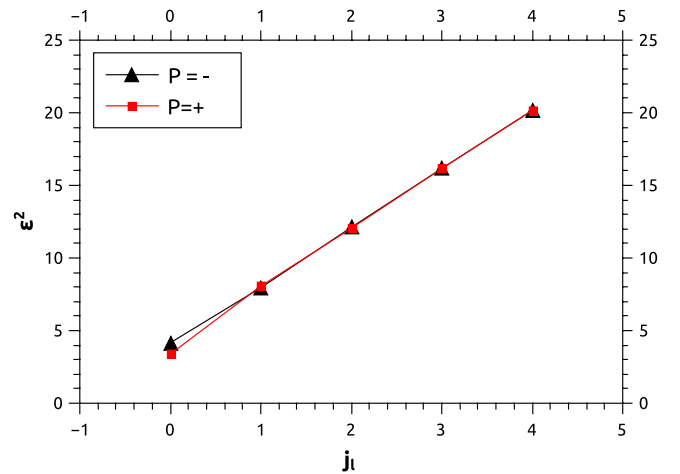
FIG. 7 (color online).   Angular Regge trajectories for the ground states, ε^2 in units of σ.
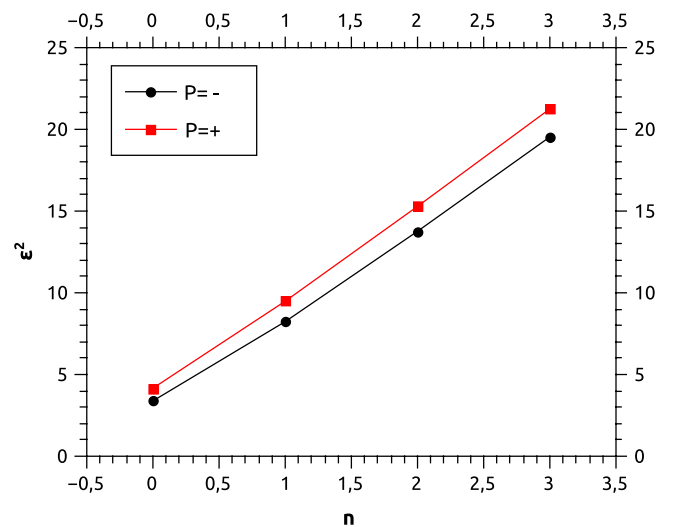
FIG. 8 (color online).   Radial Regge trajectories for chiral partners $0+\frac{1}{2}$ and $1-\frac{1}{2}$, ε^2 in units of σ.
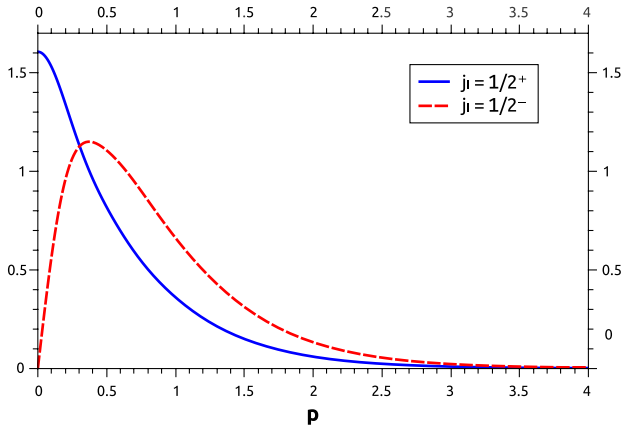
FIG. 9 (color online).   Chiral partners for $j_l = \frac{1}{2}$, n = 0.
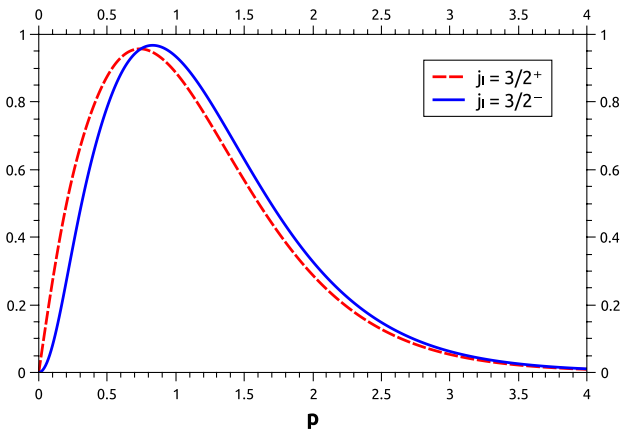
FIG. 10 (color online).   Chiral partners for $j_l = \frac{3}{2}$, n = 0.
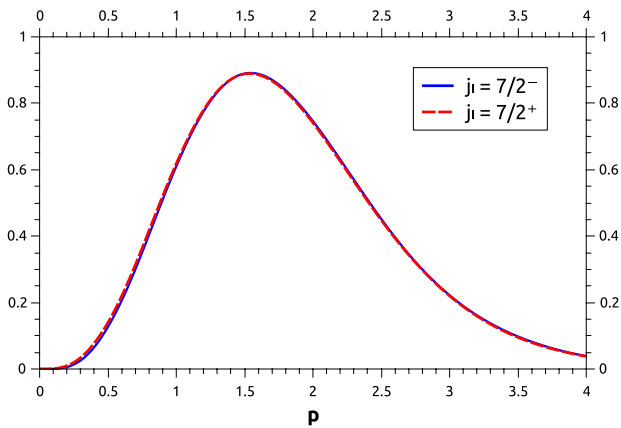
FIG. 11 (color online).   Chiral partners for $j_l = \frac{7}{2}$, n = 0.

VIII. EFFECTIVE RESTORATION OF CHIRAL SYMMETRY FOR MESONS

In the previous sections we discussed numerical aspects of the effective restoration of chiral symmetry, here we perform some more analytical considerations. The increase

of the light quark total angular momentum causes the growth of the quark relative momentum inside the meson. This can be also seen from the wave function plots, where the wave function's peaks shift to the right with the increase of j_l. Then, effectively, for high j_l only the high momenta contribute to the integrals in the Bethe-Salpeter equation. The dynamical mass $M(p)$ and chiral angle $\varphi(p)$ approach zero rather fast for $p \to \infty$ and effectively vanish in the BSE. Here we consider the consequences of such a vanishing.

In terms of notations (25)–(32) the diagonalized version of Eqs. (25)–(29) can be written as

$$A : C\vec{\psi}(p) = \begin{pmatrix} \int_q (r_- P_{J-1} + r_+ P_J) & 0 \\ 0 & \int_q (r_- P_{J+1} + r_+ P_J) \end{pmatrix}$$
$$\times \vec{\psi}(p),$$

$$B : C\vec{\psi}(p) = \begin{pmatrix} \int_q (r_+ P_{J-1} + r_- P_J) & 0 \\ 0 & \int_q (r_+ P_{J+1} + r_- P_J) \end{pmatrix}$$
$$\times \vec{\psi}(p), \qquad (38)$$

where the first and second equations describe categories A and B of mesons, respectively. When the chiral angle is set to zero, the coefficients r_+ and r_- are $r_+(\varphi = 0) = 1$, $r_-(\varphi = 0) = 1$, therefore the equations for categories A and B from (38) become identical. And the masses of the states with opposite parities must coincide, which is the direct signal of chiral restoration.

Analogous considerations are applicable to the case, where $m_1 = 0$ and m_2 is an arbitrary finite constant. Therefore, in such kind of mesons the effective restoration of chiral symmetry is also expected.

IX. CONCLUSIONS

Within a model with the linear instantaneous Coulomb-like confining potential between quark currents we have demonstrated a fast effective restoration of chiral symmetry in the spectrum of heavy-light mesons. Effective chiral restoration leads to degenerate masses of chiral partners (mesons with opposite parity) and to the corresponding degeneration in the wave functions.

Chiral symmetry breaking appears in this model in the standard way through the nonperturbative quark self-interaction, generating a nonzero dynamical mass of the light quark. The dynamical mass is momentum-dependent and vanishes at large momenta. For the heavy-light mesons with large J the typical momentum of the light quark is high, therefore it has a small effective dynamical mass and all quantum (loop) effects are suppressed in this limit.

To describe bound states of the heavy-light system we derived the Bethe-Salpeter equation for two quarks with different masses, which corresponds to a system of coupled integral equations. Then, by taking the limit $m_1 \to 0$, $m_2 \to \infty$ we obtained a heavy-light version of the equations and

proved the existence of heavy spin symmetry in this limit. When the dynamical mass is zero these equations form exact chiral multiplets (parity doublets). This is effective chiral restoration. Since the main physics is the same, the system of one quark with finite, not zero mass and one massless quark must also provide effective restoration of chiral symmetry.

ACKNOWLEDGMENTS

APPENDIX A

When the light-light mesons are constructed, they can be classified with respect to J^{PC} quantum numbers and fall into four categories [22]:

$$\text{I:}\begin{cases} J^{-+}, J = 2n \\ J^{+-}, J = 2n+1 \end{cases} \quad \text{II:}\begin{cases} J^{++}, J = 2n \\ J^{--}, J = 2n+1 \end{cases}$$

$$\text{III:}\begin{cases} J^{--}, J = 2n \\ J^{++}, J = 2n+1 \end{cases} \quad \text{IV:}\begin{cases} J^{+-}, J = 2n \\ J^{-+}, J = 2n+1. \end{cases}$$

In the case of mesons built from the quarks with different masses, the charge parity C is not a well-defined quantum number. The classification of states should be done according only to the parity P and to the angular momentum J. Then to form states with definite parity and undefined charge parity the categories I and III mix and produce category A; categories II and IV produce category B.

$$\text{A:}\begin{cases} J^{-}, J = 2n \\ J^{+}, J = 2n+1 \end{cases} \quad \text{B:}\begin{cases} J^{+}, J = 2n \\ J^{-}, J = 2n+1. \end{cases}$$

As it is pointed out in [22], the instantaneous interaction in the Bethe-Salpeter equation leads to the absence of the states of category IV in the spectrum. However, this doesn't affect the case with different quark masses and category B should be still considered as a union of categories II and IV.

The parametrizations for the vertex functions of categories A and B follow from their construction and are the sums of corresponding parametrizations of categories I, III and II, IV. Then using the formulas (A9), (A12), (A15), (A18) from [22] one can obtain the meson rest frame vertex functions for the instantaneous interaction.

The vertex function of category A is

$$\begin{aligned}
\chi^P_{JM}(m, \vec{p}) &= \gamma_5 Y_{JM}(\hat{p})\chi_1(p) + m\gamma_0\gamma_5 Y_{JM}(\hat{p})\chi_2(p) \\
&\quad + m\gamma_0\gamma_5\{Y_{J+1}(\hat{p}) \otimes \vec{\gamma}\}_{JM}\chi_3(p) \\
&\quad + m\gamma_0\gamma_5\{Y_{J-1}(\hat{p}) \otimes \vec{\gamma}\}_{JM}\chi_4(p) \\
&\quad + m\{Y_J(\hat{p}) \otimes \vec{\gamma}\}_{JM}\chi_5(p) \\
&\quad + \gamma_5\{Y_{J+1}(\hat{p}) \otimes \vec{\gamma}\}_{JM}\chi_6(p) \\
&\quad + \gamma_5\{Y_{J-1}(\hat{p}) \otimes \vec{\gamma}\}_{JM}\chi_7(p) \\
&\quad + \gamma_0\{Y_J(\hat{p}) \otimes \vec{\gamma}\}_{JM}\chi_8(p),
\end{aligned} \quad (A1)$$

where $\{\vec{a}_{J_1} \otimes \vec{b}_{J_2}\}_{JM}$ is the coupling of two spherical tensors of rank J_1 and J_2 to a spherical tensor of rank J, $Y_{JM}(\hat{p})$ are spherical harmonics and we denote $p = |\vec{p}|$. For $J = 0$ the components 4, 5, 7, 8 are absent.

The vertex function of category B is

$$\begin{aligned}
\chi^P_{JM}(m, \vec{p}) &= Y_{JM}(\hat{p})\chi_1(p) + \{Y_{J+1}(\hat{p}) \otimes \vec{\gamma}\}_{JM}\chi_2(p) \\
&\quad + \{Y_{J-1}(\hat{p}) \otimes \vec{\gamma}\}_{JM}\chi_3(p) \\
&\quad + m\gamma_5\{Y_J(\hat{p}) \otimes \vec{\gamma}\}_{JM}\chi_4(p) \\
&\quad + m\gamma_0\{Y_{J+1}(\hat{p}) \otimes \vec{\gamma}\}_{JM}\chi_5(p) \\
&\quad + m\gamma_0\{Y_{J-1}(\hat{p}) \otimes \vec{\gamma}\}_{JM}\chi_6(p) \\
&\quad + m\gamma_0 Y_{JM}(\hat{p})\chi_7(p) \\
&\quad + \gamma_0\gamma_5\{Y_J(\hat{p}) \otimes \vec{\gamma}\}_{JM}\chi_8(p).
\end{aligned} \quad (A2)$$

For $J = 0$ the components 3, 4, 6, 8 are absent.

APPENDIX B

Here we sketch the the derivation of the coupled integral Bethe-Salpeter equations for category A, since the equations for category B may be treated in the same way.

The vertex function in the rest frame doesn't depend on p_0 and it is easy to take the p_0 integral in the Bethe-Salpeter equation (23)

$$\begin{aligned}
\chi(m, \vec{p}) &= \int \frac{d^3q}{(2\pi)^3} V(k)\gamma_0 \left\{ \frac{\gamma_0\omega_1(q)+A_1(q)-\vec{\gamma}\cdot\hat{q}B_1(q)}{2\omega_1(q)} \right. \\
&\quad \times \chi(m, \vec{q}) \frac{\gamma_0(\omega_1(q)-m)+A_2(q)-\vec{\gamma}\cdot\hat{q}B_2(q)}{(\omega_1(q)-m)^2-\omega_2^2(q)} \\
&\quad + \frac{\gamma_0(\omega_2(q)+m)+A_1(q)-\vec{\gamma}\cdot\hat{q}B_1(q)}{(\omega_2(q)+m)^2-\omega_1^2(q)} \\
&\quad \left. \times \chi(m, \vec{q}) \frac{\gamma_0\omega_2(q)+A_2(q)-\vec{\gamma}\cdot\hat{q}B_2(q)}{2\omega_2(q)} \right\}\gamma_0, \quad (B1)
\end{aligned}$$

where $k = |\vec{p} - \vec{q}|$. Then we substitute the vertex meson functions $\chi^P_{JM}(m, \vec{p})$ from (A1) and (A2) to the BSE. The interaction kernel mixes the initial Dirac structures. To match left hand side BSE Dirac structures with right hand

side ones, we project out the functions $\chi_i(p)$ on the left hand side. The projection involves taking the traces of Dirac matrices and can be done by using of formulas (B1–B6) from [22]. This leads to a system of eight coupled integral equations for the basis elements χ_i. However, not all of these equations are linear independent. Introducing new functions

$$A_1(q) = \cos\varphi_-(q)\chi_1(q) - \sqrt{\frac{J+1}{2J+1}}\sin\varphi_-(q)\chi_6(q) + \sqrt{\frac{J}{2J+1}}\sin\varphi_-(q)\chi_7(q), \tag{B2}$$

$$A_2(q) = A_1(q) + 2\omega_+(q)\left\{\sin\varphi_+(q)\chi_2(q) - \sqrt{\frac{J+1}{2J+1}}\cos\varphi_-(q)\chi_3(q) + \sqrt{\frac{J}{2J+1}}\cos\varphi_+(q)\chi_4(q)\right\}, \tag{B3}$$

$$A_3(q) = \sqrt{\frac{J}{2J+1}}\cos\varphi_+(q)\chi_6(q) + \sqrt{\frac{J+1}{2J+1}}\cos\varphi_+(q)\chi_7(q) + \sin\varphi_+(q)\chi_8(q), \tag{B4}$$

$$A_4(q) = A_3(q) + 2\omega_+(q)\left\{\sqrt{\frac{J}{2J+1}}\sin\varphi_-(q)\chi_3(q) + \sqrt{\frac{J+1}{2J+1}}\sin\varphi_-(q)\chi_4(q) + \cos\varphi_-(q)\chi_5(q)\right\}, \tag{B5}$$

we end up with four coupled integral equations,

$$A_1(p) = \frac{1}{2}\int\frac{d^3q}{(2\pi)^3}V(k)\left\{\left[\cos\varphi_-(p)\cos\varphi_-(q)P_J(\hat{p}\cdot\hat{q}) + \sin\varphi_-(p)\sin\varphi_-(q)\frac{(J+1)P_{J+1}(\hat{p}\cdot\hat{q}) + JP_{J-1}(\hat{p}\cdot\hat{q})}{2J+1}\right]\right.$$
$$\times\left[\frac{A_1(q)}{\omega_+(q)} + \frac{m^2}{4\omega_+(q)}\frac{A_2(q)}{\omega_+^2 - \frac{m^2}{4}}\right] - \sin\varphi_-(p)\cos\varphi_+(q)\frac{\sqrt{J(J+1)}}{2J+1}[P_{J+1}(\hat{p}\cdot\hat{q}) - P_{J-1}(\hat{p}\cdot\hat{q})]$$
$$\left.\times\left[\frac{A_3(q)}{\omega_+(q)} + \frac{m^2}{4\omega_+(q)}\frac{A_4(q)}{\omega_+^2 - \frac{m^2}{4}}\right]\right\} \tag{B6}$$

$$A_2(p) = A_1(p) + \frac{\omega_+(p)}{2}\int\frac{d^3q}{(2\pi)^3}V(k)\left\{\left[\sin\varphi_+(p)\sin\varphi_+(q)P_J(\hat{p}\cdot\hat{q})\right.\right.$$
$$\left.+ \cos\varphi_+(p)\cos\varphi_+(q)\frac{(J+1)P_{J+1}(\hat{p}\cdot\hat{q}) + JP_{J-1}(\hat{p}\cdot\hat{q})}{2J+1}\right]\times\frac{A_2(q)}{\omega_+^2 - \frac{m^2}{4}} - \cos\varphi_+(p)\sin\varphi_-(q)\frac{\sqrt{J(J+1)}}{2J+1}$$
$$\left.\times[P_{J+1}(\hat{p}\cdot\hat{q}) - P_{J-1}(\hat{p}\cdot\hat{q})]\frac{A_4(q)}{\omega_+^2 - \frac{m^2}{4}}\right\} \tag{B7}$$

$$A_3(p) = \frac{1}{2}\int\frac{d^3q}{(2\pi)^3}V(k)\left\{\left[\sin\varphi_+(p)\sin\varphi_+(q)P_J(\hat{p}\cdot\hat{q}) + \cos\varphi_+(p)\cos\varphi_+(q)\frac{JP_{J+1}(\hat{p}\cdot\hat{q}) + (J+1)P_{J-1}(\hat{p}\cdot\hat{q})}{2J+1}\right]\right.$$
$$\times\left[\frac{A_3(q)}{\omega_+(q)} + \frac{m^2}{4\omega_+(q)}\frac{A_4(q)}{\omega_+^2 - \frac{m^2}{4}}\right] - \cos\varphi_+(p)\sin\varphi_-(q)\frac{\sqrt{J(J+1)}}{2J+1}[P_{J+1}(\hat{p}\cdot\hat{q}) - P_{J-1}(\hat{p}\cdot\hat{q})]$$
$$\left.\times\left[\frac{A_1(q)}{\omega_+(q)} + \frac{m^2}{4\omega_+(q)}\frac{A_2(q)}{\omega_+^2 - \frac{m^2}{4}}\right]\right\} \tag{B8}$$

$$A_4(p) = A_3(p) + \frac{\omega_+(p)}{2}\int\frac{d^3q}{(2\pi)^3}V(k)\left\{\left[\cos\varphi_-(p)\cos\varphi_-(q)P_J(\hat{p}\cdot\hat{q})\right.\right.$$
$$\left.+ \sin\varphi_-(p)\sin\varphi_-(q)\frac{JP_{J+1}(\hat{p}\cdot\hat{q}) + (J+1)P_{J-1}(\hat{p}\cdot\hat{q})}{2J+1}\right]$$
$$\left.\times\frac{A_4(q)}{\omega_+^2 - \frac{m^2}{4}} - \sin\varphi_-(p)\cos\varphi_+(q)\frac{\sqrt{J(J+1)}}{2J+1}\times[P_{J+1}(\hat{p}\cdot\hat{q}) - P_{J-1}(\hat{p}\cdot\hat{q})]\frac{A_2(q)}{\omega_+^2 - \frac{m^2}{4}}\right\}, \tag{B9}$$

where $\omega_+(p) = \frac{1}{2}(\omega_1(p) + \omega_2(p))$ and $\varphi_\pm(p) = \frac{1}{2}(\varphi_1(p) \pm \varphi_2(p))$.

The equations above lead to the equations for heavy-light mesons if we define a wave function as (see Appendix C)

$$\psi_{i,\pm}(p) = \frac{1}{2}\left[h_i(p) \pm \frac{m}{2}\left(1 \pm \frac{m}{2\omega_+(p)}\right)g_i(p)\right], \quad (B10)$$

where

$$h_1(p) = \frac{A_1(p)}{\omega_+(p)}, \quad (B11)$$

$$g_1(p) = \frac{A_2(p)}{\omega_+^2(p) - \frac{m^2}{4}}, \quad (B12)$$

$$h_2(p) = \frac{A_3(p)}{\omega_+(p)} \quad (B13)$$

$$g_2(p) = \frac{A_4(p)}{\omega_+^2(p) - \frac{m^2}{4}}. \quad (B14)$$

APPENDIX C

We derive the rest frame wave function and its projections on the components propagating backward and forward in time [40].

The wave function in the rest frame is

$$\psi_{JM}^P(m, \vec{p}) = i \int \frac{dp_0}{2\pi} S_1\left(p_0 + \frac{m}{2}, \vec{p}\right)$$
$$\times \chi_{JM}^P(m, \vec{p}) S_2\left(p_0 - \frac{m}{2}, \vec{p}\right).$$

The quark propagator can be splitted into

$$S(p_0, \vec{p}) = S_+(p_0, \vec{p}) + S_-(p_0, \vec{p}), \quad (C1)$$

where

$$S_\pm(p_0, \vec{p}) = i\frac{T_p P_\pm T_p^\dagger \gamma_0}{p_0 \mp \omega(p) \pm i\epsilon}, \quad (C2)$$

$$T_p = \exp\left[-\frac{1}{2}\vec{\gamma} \cdot \hat{p}\left(\frac{\pi}{2} - \varphi_p\right)\right] \quad (C3)$$

and projectors are

$$P_\pm = \frac{1 \pm \gamma_0}{2}. \quad (C4)$$

The integration over p_0 may be performed with the help of equalities $P_\pm\gamma_0 = \pm P_\pm$, $T_p^\dagger\gamma_0 = \gamma_0 T_p$ and leads to

$$\psi_{JM}^P(m, \vec{p}) = \frac{T_{p,1}P_+T_{p,1}\chi_{JM}^P(m, \vec{p})T_{p,2}P_-T_{p,2}}{2\omega_+(p) - m}$$
$$+ \frac{T_{p,1}P_-T_{p,1}\chi_{JM}^P(m, \vec{p})T_{p,2}P_-T_{p,2}}{2\omega_+(p) + m}. \quad (C5)$$

Since $T_p^\dagger = T_p^{-1}$, the Foldy transformation of the wave function $\tilde{\psi}_{JM}^P(m, \vec{p}) = T_{p,1}^\dagger\psi_{JM}^P(m, \vec{p})T_{p,2}^\dagger$ is

$$\tilde{\psi}_{JM}^P(m, \vec{p}) = P_+\psi_{+JM}^P(m, \vec{p})P_- + P_-\psi_{-JM}^P(m, \vec{p})P_+, \quad (C6)$$

where '+' and '−' components correspond to the propagation forward and backward, respectively. The result for the forward and backward propagating wave function for category A is

$$\psi_{\pm JM}^P(m, \vec{p}) = \psi_{1,\pm}(p)\gamma_5 Y_J(\hat{p})$$
$$\pm \psi_{2,\pm}(p)\{Y_J(\hat{p}) \times \vec{\gamma}\}_{JM}. \quad (C7)$$

For category B, the wave functions obey

$$\psi_{\pm JM}^P(m, \vec{p}) = \left[\sqrt{\frac{J}{2J+1}}\psi_{1,\pm}(p) + \sqrt{\frac{J+1}{2J+1}}\psi_{2,\pm}(p)\right]$$
$$\times \{Y_{J+1}(\hat{p}) \times \vec{\gamma}\}_{JM}$$
$$+ \left[\sqrt{\frac{J+1}{2J+1}}\psi_{1,\pm}(p) - \sqrt{\frac{J}{2J+1}}\psi_{2,\pm}(p)\right]$$
$$\times \{Y_{J-1}(\hat{p}) \times \vec{\gamma}\}_{JM}. \quad (C8)$$

The wave function components for both categories $\psi_{i,\pm}(p)$ are defined as

$$\psi_{i,\pm}(p) = \frac{1}{2}\left[h_i(p) \pm \frac{m}{2}\left(1 \pm \frac{m}{2\omega_+(p)}\right)g_i(p)\right]. \quad (C9)$$

APPENDIX D

Here we present a procedure for the numerical solution of the heavy-light BSE. The binding energy spectrum and meson wave functions were calculated for three different values of the infrared regulator $\mu_{IR} = 0.01\sqrt{\sigma}$, $\mu_{IR} = 0.005\sqrt{\sigma}$ and $\mu_{IR} = 0.001\sqrt{\sigma}$. The final results were obtained by extrapolation to the infrared limit $\mu_{IR} \to 0$, see Fig. 12.

The chiral angle and the single quark energy, inputs to the BSE, are obtained from the iterative solution of the gap equation.

Taking into account the diagonalization (Sec. IV), the Bethe-Salpeter equation for an arbitrary J may be viewed as

$$(H(p|\omega(p)) + \epsilon)\psi(p) = \int dq F(p, q|\varphi(p), \varphi(q))\psi(q), \quad (D1)$$
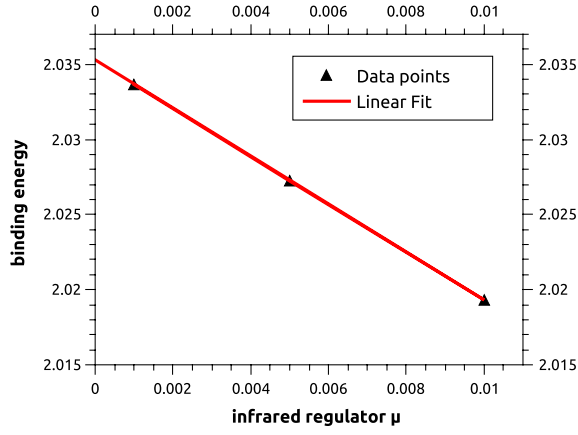
FIG. 12 (color online). Calculated data points, linear fit.

where $\varphi(p)$ is the chiral angle, $\omega(p)$ is the single quark energy and $\psi(p)$ is the wave function. We solve equations of this kind by expanding the unknown wave function in the basis

$$\psi(p) = \sum_{i=1}^{N} C_i \xi_i(p). \qquad (D2)$$

To match the appropriate boundary conditions, we choose

$$\xi_i(p) = p^J \exp(-\alpha_i p^2) \qquad (D3)$$

for the mesons of category A and

$$\xi_i(p) = p^{|J-1|} \exp(-\alpha_i p^2) \qquad (D4)$$

for the mesons of category B. It is enough to use a relatively small number of Gaussians for a sufficient accuracy of the expansion. Then the truncated equation (D1) becomes a system of linear equations,

$$(H(p|\omega(p)) + \epsilon) \sum_{i=1}^{N} C_i \xi_i(p)$$

$$= \int dq F(p, q|\varphi(p), \varphi(q)) \sum_{i=1}^{N} C_i \xi_i(q). \qquad (D5)$$

Multiplying (D5) by $\xi_j(p)$ and integrating over p, we end up with the generalized eigenvalue problem,

$$\epsilon D \vec{C} = (A + B) \vec{C}, \qquad (D6)$$

where

$$D_{ij} = \int dp \xi_i(p) \xi_j(p),$$

$$A_{ij} = \int dp \xi_i(p) \xi_j(p) H(p|\omega(p)),$$

$$B_{ij} = \int dp \int dq \xi_i(p) \xi_j(q) F(p, q|\varphi(p), \varphi(q)).$$

The solution of the problem (D6) leads to the spectrum of binding energies and to the corresponding meson wave functions.

[1] V. Koch, arXiv:nucl-th/9512029.

[2] S. L. Adler, Phys. Rev. **177**, 2426 (1969).

[3] J. Bell and R. Jackiw, Nuovo Cimento A **60**, 47 (1969).

[4] K. Fujikawa, Phys. Rev. Lett. **42**, 1195 (1979).

[5] M. Gell-Mann and M. Levy, Nuovo Cimento **16**, 705 (1960).

[6] C. B. Lang and M. Schrock, Phys. Rev. D **84**, 087704 (2011).

[7] M. Schrock, Phys. Lett. B **711**, 217 (2012).

[8] L. Y. Glozman, C. B. Lang, and M. Schrock, Phys. Rev. D **86**, 014507 (2012).

[9] L. Y. Glozman, Phys. Lett. B **475**, 329 (2000).

[10] T. D. Cohen and L. Y. Glozman, Phys. Rev. D **65**, 016006 (2001).

[11] T. D. Cohen and L. Y. Glozman, Int. J. Mod. Phys. A **17**, 1327 (2002).

[12] L. Y. Glozman, Phys. Lett. B **541**, 115 (2002).

[13] L. Y. Glozman, Phys. Lett. B **539**, 257 (2002).

[14] L. Y. Glozman, Phys. Lett. B **587**, 69 (2004).

[15] L. Y. Glozman, Int. J. Mod. Phys. A **21**, 475 (2006).

[16] L. Y. Glozman, Phys. Rep. **444**, 1 (2007).

[17] L. Y. Glozman, A. V. Nefediev, and J. E. F. T. Ribeiro, Phys. Rev. D **72**, 094002 (2005).

[18] A. Le Yaouanc, L. Oliver, O. Pène, and J.-C. Raynal, Phys. Rev. D **29**, 1233 (1984).

[19] A. Le Yaouanc, L. Oliver, S. Ono, O. Pène, and J.-C. Raynal, Phys. Rev. D **31**, 137 (1985).

[20] Y. S. Kalashnikova, A. V. Nefediev, and J. E. F. T. Ribeiro, Phys. Rev. D **72**, 034020 (2005).

[21] R. F. Wagenbrunn and L. Y. Glozman, Phys. Lett. B **643**, 98 (2006).

[22] R. F. Wagenbrunn and L. Y. Glozman, Phys. Rev. D **75**, 036007 (2007).

[23] S. Afonin, Eur. Phys. J. A **29**, 327 (2006).

[24] M. Shifman, in *Proceedings of the First Workshop on Quark-Hadron Duality and the Transition to pQCD, Frascati, Italy, 2005,* edited by A. Fantoni, S. Liuti, and A. O. Rondon-Aramayo (World Scientific, Singapore, 2006).

[25] O. Catà, M. Golterman, and S. Peris, Phys. Rev. D **74**, 016001 (2006).

[26] T. DeGrand, Phys. Rev. D **69**, 074024 (2004).

[27] E. S. Swanson, Phys. Lett. B **582**, 167 (2004).

[28] N. Ligterink and E. S. Swanson, Phys. Rev. C **69**, 025204 (2004).

[29] T. D. Cohen, Nucl. Phys. **A775**, 89 (2006).

[30] Y. Nakagawa, A. Voigt, E.-M. Ilgenfritz, M. Müller-Preussker, A. Nakamura, T. Saito, A. Sternbeck, and H. Toki, Phys. Rev. D **79**, 114504 (2009).

[31] N. Isgur and M. B. Wise, Phys. Lett. B **232**, 113 (1989).

[32] J. Flynn and N. Isgur, J. Phys. G **18**, 1627 (1992).

[33] W. A. Bardeen and C. T. Hill, Phys. Rev. D **49**, 409 (1994).

[34] W. A. Bardeen, E. J. Eichten, and C. T. Hill, Phys. Rev. D **68**, 054024 (2003).

[35] G. 't Hooft, Nucl. Phys. **B72**, 461 (1974).

[36] G. 't Hooft, Nucl. Phys. **B75**, 461 (1974).

[37] S. L. Adler and A. Davis, Nucl. Phys. **B244**, 469 (1984).

[38] R. Alkofer and P. Amundsen, Nucl. Phys. **B306**, 305 (1988).

[39] L. Y. Glozman, V. K. Sazonov, M. Shifman, and R. F. Wagenbrunn Phys. Rev. D **85**, 094030 (2012).

[40] L. Y. Glozman and A. V. Nefediev, Phys. Rev. D **73**, 074018 (2006).